# Cyclic Fatigue Testing and Metallographic Analysis of Nickel-Titanium Rotary Instruments

*Chiara Pirani, DDS, MS, PhD,* Pier Paolo Cirulli, DDS,* Stefano Chersoni, DDS, MS, PhD,* Lorenzo Micele, DSc, PhD,† Oddone Ruggeri, DSc,† and Carlo Prati, MD, DDS, PhD**

## Abstract

**Introduction:** The aim of this study was to compare cyclic fatigue resistance of four nickel-titanium rotary systems and to evaluate their surface, fractographic, and matrix morphology. **Methods:** Four models of endodontic rotary files (EasyShape [Komet/Gebr. Brasseler, Lemgo, Germany], ProTaper [Dentsply Maillefer, Ballaigues, Switzerland], NRT [MANI Inc, Toshigi-Ken, Japan], and AlphaKite [Komet/Gebr. Brasseler]) were subjected to fatigue testing in artificial canals with angle of curvature of 45° and 60° and a radius of curvature of 5 mm until fracture occurred. Nickel-titanium (NiTi) alloy properties were investigated by light microscopy, environmental scanning electron microscopy (ESEM), and energy dispersive x-ray spectrophotometry (EDS). ESEM analysis was conducted on new files to examine surface characteristics and on fractured samples to identify the crack origin and the fractographic features. **Results:** Analysis of variance testing revealed significant differences ($P < .001$) among the groups. NRT files had the highest fatigue resistance followed by AlphaKite, EasyShape, and ProTaper. All the new files presented surface imperfections. Fractographic analysis found the crack initiation to originate at the level of surface irregularities. Optical microscope inspection of the NiTi alloy matrix disclosed different-sized nonmetallic inclusions among models. EDS analysis of these inclusions showed that they were composed of carbon and oxygen in addition to nickel and titanium. Under light microscopy, austenitic grains appeared larger near the handle and smaller near the tip in all instruments. **Conclusions:** NRT files presented the longest fatigue life. All samples showed surface irregularities and nonmetallic inclusions. Austenitic grains were smaller near the tip than near the handle. The angle of curvature was confirmed to influence the fatigue life of NiTi instruments. *(J Endod 2011;37:1013–1016)*

## Key Words

Cyclic fatigue, environmental scanning electron microscope, fracture, NiTi instruments, TiN coating

Nickel-titanium (NiTi) root canal files were first introduced in 1988 by Walia et al (1) to overcome the rigidity of stainless steel instruments and thereby improve the instrumentation of curved canals (1). NiTi is far more flexible than stainless steel, and its superelasticity reduces the restoring force (2), thereby allowing improved canal shaping and reduced transportation (3). Despite the many advantages of NiTi instrumentation, unexpected fractures may occur during clinical use (4, 5), and the impairment of the outcome of root canal treatment results from the impossibility of removing the instrument (5). According to Sattapan et al (6), two different separation mechanisms occur in rotary instruments: torsional (ductile) and fatigue (brittle) fracture. Instruments separated by torsional stresses usually present macroscopic plastic deformation (7), whereas instruments fractured by fatigue generally exhibit no specific macroscopic pattern (6).

Although several clinical and laboratory studies have investigated the cumulative effects of multiple tensile-compressive stresses on the incidence of cyclic fatigue and instrument separation for NiTi files (5, 6, 8, 9), little is known on how surface and alloy features affect NiTi instrument fracture.

The aim of the present study was to compare the cyclic fatigue resistance of NiTi endodontic rotary files in simulated 45° and 60° curved canals and to correlate their fatigue life with their surface, matrix, and fractographic features. The tested null hypothesis was that there are no differences between the NiTi instruments examined.

## Materials and Methods

The cyclic fatigue testing was conducted in a manner similar to that performed by Lopes et al (10, 11). Two 16-G stainless steel needles (LG Forniture, Osimo, Italy) were bent to obtain artificial canals with a 5-mm radius of curvature, curvature angles of 45° and 60°, and an overall length of 22. NiTi instruments were tested for cyclic fatigue in a stainless steel apparatus composed of a base and a vertical axis. The vertical axis contained a structure that allowed the movement of the 16:1 reduction handpiece powered by a torque-controlled electric stepper motor (Xsmart; Dentsply Maillefer, Baillagues, Switzerland). At the apparatus base, a bench vise was used to hold the artificial canals. This device ensured standardized placement of the NiTi instruments in the artificial canals. All the instruments were mounted on the electrical handpiece and were inserted 22 mm into the steel canal. A silicone stop (Endo Stopper, Kumapan, Bourges, France) was mounted on each instrument to easily mark the correct length of the part introduced into the artificial canal.

From the Departments of *Dental Sciences, Alma Mater Studiorum; and †Metal Sciences, Electrochemistry and Chemical Techniques, Alma Mater Studiorum, University of Bologna, Bologna, Italy.

Address requests for reprints to Dr Chiara Pirani, Department of Dental Sciences, Alma Mater Studiorum, University of Bologna, Via San Vitale 59, 40125 Bologna, Italy. E-mail address: chiara.pirani4@unibo.it

0099-2399/$ - see front matter



doi:10.1016/j.joen.2011.04.009

**TABLE 1.** Mean and Standard Deviation of the Number of Cycles to Fracture for Each Group at 45° and at 60°

| | NRT | ProTaper | EasyShape | AlphaKite |
|---|---|---|---|---|
| 45° | 3923.1 ± 192.4 | 2746.7 ± 109.1 | 3010.1 ± 299 | 3361.8 ± 236.9 |
| 60° | 957.7 ± 59.2 | 571.5 ± 92.3 | 704.9 ± 70.3 | 782.3 ± 62.4 |

The electrical handpiece was standardized to rotate the instruments at a nominal speed of 300 rpm, with a maximum torque of 3 N/Cm. Cyclic fatigue testing was conducted on four different groups (n = 22) of instruments: (1) group A: Mani NRT 25/.06 (MANI Inc, Toshigi-Ken, Japan), (2) group B: ProTaper Universal F2 (Dentsply Maillefer, Ballaigues, Switzerland), (3) group C: EasyShape 25/.06 (Komet/Gebr. Brasseler, Lemgo, Germany), and (4) group D: AlphaKite 25/.06 (Komet/Gebr. Brasseler).

Files were divided into eight subgroups (n = 11) and tested in the curved 45° and 60° artificial canals until fracture occurred. Time to fracture was recorded visually with a 1/100-second digital stopwatch (Oregon Scientific SL928D, Tualatin, OR). During the test, the stainless steel artificial canals were filled with glycerine to reduce the friction of the instrument against the canal walls.

Results were analyzed statistically using SPSS software (SPSS, Oakbrook, IL). One-way and two-way analysis of variance (ANOVA) and Tukey Honestly Significant Difference (HSD) test were calculated to determine any statistical difference amongst groups. The significance was determined at the 95% confidence level.

Fractured fragments were collected and analyzed under ESEM (EVO50 EP; Carl Zeiss NTS GmbH, Oberkochen, Germany) with magnification ranging from 400× to 10,000×. Unused instruments were examined for surface details under ESEM with magnification ranging from 100× to 5,000× at the tip and 4 mm from the tip. Each sample was then embedded in epoxy resin, wet ground with 180 to 320 grit size silicon carbide (SiC) papers, and polished with a 9-$\mu$m diamond paste. Specimens were then etched with 60% nitric acid, 10% fluorhydric acid, and 30% acetic acid at room temperature for 5 seconds (12) to disclose the microstructure of the NiTi matrix. All the etched samples were examined with an optical microscope (Zeiss AXIO, Carl Zeiss NTS GmbH) and analyzed with ESEM equipped with EDS (EDS Oxford Inca Energy 350; Oxford Instruments, Abingdon, Oxfordshire, UK).

The images of the new and fractured samples were examined in a double-blind manner by two trained operators; a consensus was reached between the two examiners regarding any discrepancies.

## Results

The mean and standard deviation of the number of cycles to fracture for each group are listed in Table 1. One-way ANOVA analysis revealed significant differences between all g roups tested, both at 45° and 60° ($P < .001$). The Tukey HSD test showed that there were significant differences between all groups at 45° and at 60° ($P < .001$) except between groups C and D at 60° ($P = .077$).

Two-way ANOVA analysis and its post hoc test (Tukey HSD) showed how every tested instrument broke significantly earlier in the 60° artificial curved canal than in the 45° curved canal ($P < .001$). It confirmed the results of one-way analysis and showed significant differences between all the combinations for 45° and 60° ($P < .001$), except between groups B and C at 60° ($P = .003$) and between groups C and D at 60° ($P = .370$).

The crack origin in every sample was identified to be at the level of superficial manufacturing defects, mainly milling grooves (Fig. 1*A*). At high magnification, fatigue striations were found close to the crack initiation area (Fig. 1*B*). Far from the crack initiation site, a dimpled surface was observed, indicating ductile fracture in which breakage occurred after plastic deformation. Dimples were similar in size and density in all models except Mani Files in which they were more numerous and shallow. In all samples examined, microvoids and inclusions were detected in proximity of the dimple centers (Fig. 1*C*).

ESEM analysis of unused instruments disclosed surface defects such as debris, pits, metal strips, longitudinal scratches, and milling grooves in all samples (Fig. 1*D*). A comparative observation of the presence and size of milling grooves, notches of the cutting edges, cavities, and scratches revealed that NRT files presented a smoother surface than ProTaper, EasyShape, and AlphaKite files.

Optical microscope observations of etched surfaces indicated inclusions randomly distributed in the matrix of the NiTi alloy of all instruments examined (Fig. 1*E* and *F*). Differences were found comparing the inclusions in the four different models of files; although ProTaper, AlphaKite, and EasyShape files showed much the same size and density of inclusions, Mani Files presented smaller inclusions with a much greater density.

Observation of the etched instruments at low magnification disclosed the austenitic grains of the NiTi alloy matrix. Austenitic grains appeared larger in the portion of the instrument near the handle (Fig. 1*G*) and smaller near the tip of the file (Fig. 1*H*) in all samples.

The EDS analysis conducted on the inclusions showed their chemical composition, disclosing carbon and oxygen in addition to nickel and titanium, whereas EDS analysis of the NiTi matrix confirmed a composition of roughly 55% nickel and 45% titanium.

## Discussion

The fracture process of rotary NiTi files is of clinical interest because instrument separation may impair clinical outcomes given the difficulty in removing the separated file (13). A disadvantage of NiTi alloy is its low ultimate tensile and yield strength compared with stainless steel, making it more susceptible to fracture at lower loads (14).

The tested null hypothesis was rejected. The results of the present study revealed that NRT files resisted fatigue fracture for a longer time, showing higher flexural strength, whereas ProTaper F2 resisted significantly less time than the other instruments. Cycles to fracture decrease as the diameter of the instrument increases (15, 16). ProTaper F2 has a variable taper, .08 from D1 to D3 and .06 from D4 to D14. A diameter of 0.55 mm was calculated to be at 4 mm from the tip in ProTaper, whereas in AlphaKite, EasyShape, and NRT files, the same diameter was at 5 mm.

As described by Pruett et al (15), the maximum area of stress in the instrument is close to the arc midpoint of the canal. In the present study, this area was approximately at 4 to 5 mm from the tip of the artificial canal. Because every instrument at this level has a comparable diameter, the instruments could be compared.

Test results corroborated the conclusion that the canal curvature angle with the same radius influences the cyclic fatigue resistance of NiTi instruments. The greater the angle of curvature, the lower the number of cycles the endodontic files can tolerate until fracture occurs (17).

Crystalline materials always contain inclusions within the grains or the grain boundaries. Under the influence of an applied load, these inclusions may fracture or debond, producing pores or voids (18). Ounsi et al (19) observed voids in the fracture surface of NiTi files, assuming them to be caused by the Kirkendall effect. In the micrographs

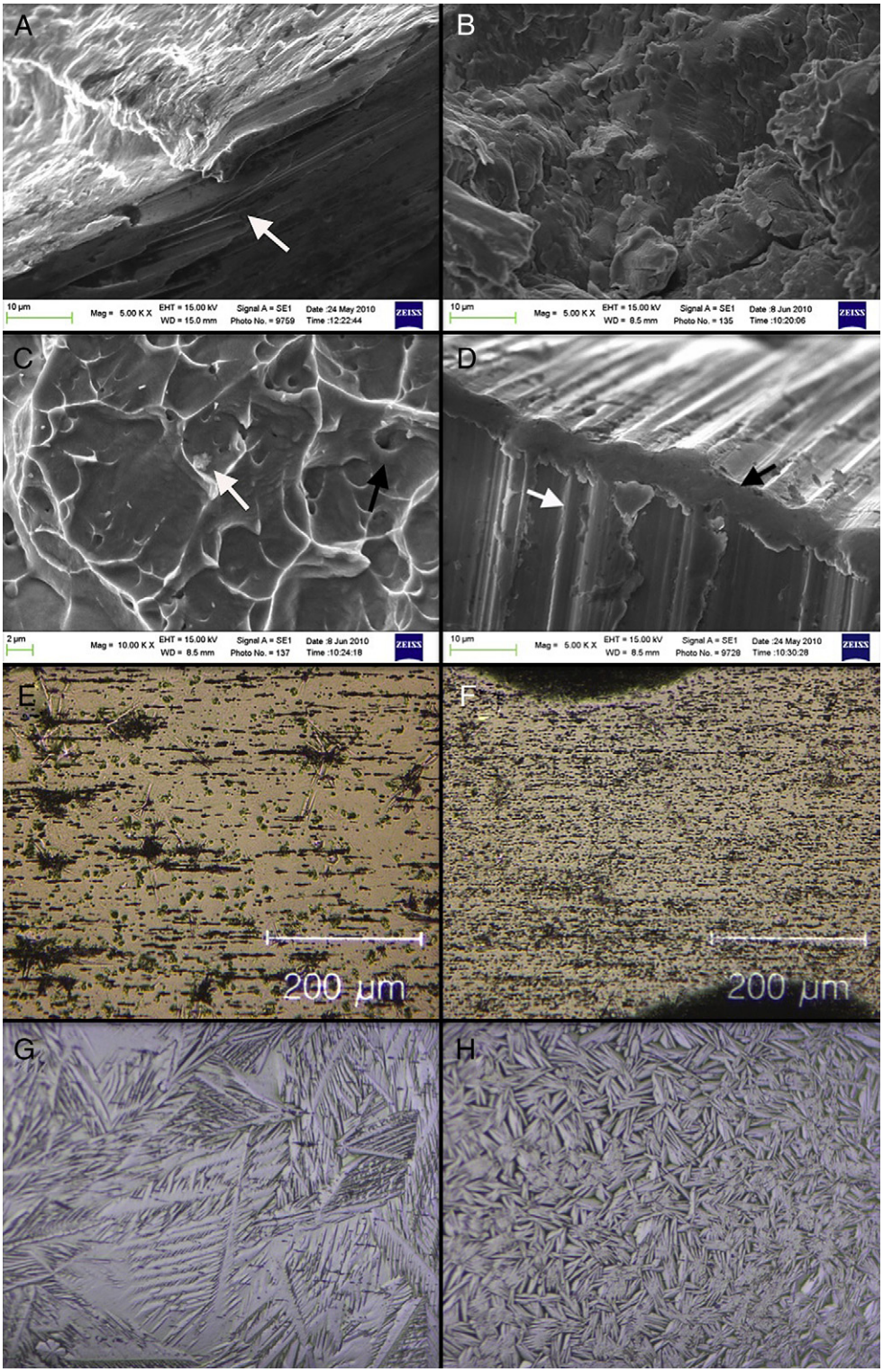


**Figure 1.** (*A*) A micrograph (5,000×) of the crack initiation site. The milling groove from which the fracture originated (*white arrow*) is visible. Parallel striations typical of cyclic fatigue are detectable. (*B*) A micrograph (5,000×) showing fatigue striations. (*C*) A high-magnification (10,000×) micrograph of dimpled surface. Holes (*black arrow*) and inclusions (*white arrow*) are evident. (*D*) A high-magnification (5,000×) micrograph of the cutting edge of a ProTaper Universal F2 with deep milling grooves (*white arrow*), metal rollover, and notching of the cutting blade (*black arrow*). (*E*) A micrograph of lattice inclusions in a Komet file. (*F*) A micrograph of lattice inclusions in a Mani File. The inclusions are smaller and have greater density compared with other instruments. (*G*) An optical micrograph of the austenitic grains of the lattice of an EasyShape file at the handle. (*H*) An optical micrograph of the austenitic grains of the lattice of an EasyShape file at the tip; the grain size progressively decreases from the handle to the tip of the instrument.

examined in the present work, inclusions were often found at the level of these pores, suggesting instead they could be produced by the debonding of nonmetallic inclusions. ESEM, EDS, and optical microscope analysis were performed on these inclusions. The inclusions are assumed to be essentially titanium carbides and NiTi oxides ($Ti_4Ni_2O_x$) formed during vacuum melting of NiTi alloy in a graphite crucible (20, 21). Because inclusions in NRT files are much more concentrated and smaller than those in the other models, this may suggest differences in the manufacturing method. It is well known that crack propagation is much enhanced by large nonmetallic inclusions acting as nucleation sites of void in ductile fracture (22, 23). By contrast, small inclusions could slow or stop propagation of the crack acting as pinning points. A pinning point in the material serves to halt a dislocation movement, requiring a greater amount of force to be applied to overcome the barrier (24).

The austenitic grain size of the NiTi alloy can also influence crack propagation. Crack nucleation along grain boundaries caused by locally concentrated stress is known to subside with decreasing grain size. Therefore, a smaller grain size can increase the yield strength of a metal (18). All the samples in this study showed smaller austenitic grains near the tip where the stresses are mostly concentrated and the risk of fracture is higher. It is possible that the swaging process of the NiTi wire could have compressed the austenitic grains, thereby producing smaller grains.

Examination of unused files showed structural defects and imperfections in all samples. The surface of the instruments showed cavities, debris, longitudinal scratches, irregular cutting edges, and milling marks. These defects may weaken the cutting efficiency of the instruments and make them more vulnerable to fracture (25), serving as notches that would concentrate the stress (26, 27). The fractographic analysis conducted in this work seemed to confirm the influence of superficial defects as an important aspect in the resistance of NiTi files, at least in terms of the fatigue life of the instruments. In fact, almost every file examined showed a crack initiation site at the level of a superficial defect. These findings indicate that a smoother surface could improve fatigue life resistance, and the use of electropolishing procedures has been suggested (28) to produce a surface with fewer structural defects that could enhance fracture resistance.

Our results lead to the consideration that surface and alloy features of NiTi instruments should be considered as fundamental characteristics that can influence fatigue resistance of the files. Thus, the quantity of superficial defects should be reduced during manufacturing processes, and the quality of the NiTi alloy should be improved in order to obtain a diminished risk of fracture.

In conclusion, the four different brands of NiTi rotary instruments presented similar fractographic characteristics and mechanical behavior, which is typical of metals being subjected to fatigue loads. There are significant differences in the fatigue resistance of the files tested, probably because of the different surface and alloy features.

## Acknowledgments

*The authors thank Dr Antonio Manzo for statistical analysis and Dr Iuri Boromei of SMETEC for scanning election microscopy.*

*The authors deny any conflicts of interest related to this study.*

## References

1. Walia HM, Brantley WA, Gerstein H. An initial investigation of the bending and torsional properties of Nitinol root canal files. J Endod 1988;14:346–51.
2. Peters OA. Current challenges and concepts in the preparation of root canal systems: a review. J Endod 2004;30:559–67.
3. Gergi R, Rjeily JA, Sader J, Naaman A. Comparison of canal transportation and centering ability of twisted files, Pathfile-ProTaper system, and stainless steel hand K-files by using computed tomography. J Endod 2010;36:904–7.
4. Kosa DA, Marshall G, Baumgartner JC. An analysis of canal centering using mechanical instrumentation techniques. J Endod 1999;25:441–5.
5. Parashos P, Gordon I, Messer HH. Factors influencing defects of rotary nickel-titanium endodontic instruments after clinical use. J Endod 2004;30: 722–5.
6. Sattapan B, Nervo GJ, Palamara JEA, Messer HH. Defects in rotary nickel-titanium files after clinical use. J Endod 2000;26:161–5.
7. Yum J, Cheung GS, Park JK, Hur B, Kim HC. Torsional strength and toughness of nickel-titanium rotary files. J Endod 2011;37:382–6.
8. Zelada G, Varela P, Martin B, Bahìllo JG, Magàn F, Ahn S. The effect of rotational speed and the curvature of root canals on the breakage of rotary endodontic instruments. J Endod 2002;28:540–2.
9. Spanaki-Voreadi AP, Kerezoudis NP, Zinelis S. Failure mechanism of ProTaper nickel-titanium rotary instruments during clinical use: fractographic analysis. Int Endod J 2006;39:171–8.
10. Lopes HP, Ferreira AA, Elias CN, Moreira EJ, de Oliveira JC, Siqueira JF Jr. Influence of rotational speed on the cyclic fatigue of rotary nickel-titanium endodontic instruments. J Endod 2009;35:1013–6.
11. Lopes HP, Elias CN, Vieira VT, et al. Effects of electropolishing surface treatment on the cyclic fatigue resistance of BioRace nickel-titanium rotary instruments. J Endod 2010;36:1653–7.
12. Gallardo JM, Herrera EJ, Gümpel P, Strittmatter J. Metallographic characterization of a NiTiCu shape memory alloy. Praktische Metallographie 1999;36: 594–608.
13. Crump MC, Natkin E. Relationship of broken root canal instruments to endodontic case prognosis: a clinical investigation. J Am Dent Assoc 2002; 80:1341–7.
14. Parashos P, Messer HH. Rotary NiTi instruments fracture and its consequences. J Endod 2006;32:1031–43.
15. Pruett JP, Clement DJ, Carnes DL. Cyclic fatigue testing of nickel-titanium endodontic instruments. J Endod 1997;23:77–85.
16. Gambarini G. Cyclic fatigue of nickel-titanium rotary instruments after clinical use with low- and high-torque endodontic motors. J Endod 2001;27: 772–4.
17. Zelada G, Varela P, Martìn B, Bahìllo JG, Magàn F, Ahn S. The effect of rotational speed on root canals on the breakage of rotary endodontic instruments. J Endod 2002;28:540–2.
18. ASM Handbook Volume 12: Fractography. Materials Park, OH: ASM International; 1987.
19. Ounsi HF, Al-Shalan T, Salameh Z, Grandini S, Ferrari M. Quantitative and qualitative elemental analysis of different nickel-titanium rotary instruments by using scanning electron microscopy and energy dispersive spectroscopy. J Endod 2008;34:53–5.
20. Alexandrou G, Chrissafis K, Vasiliadis L, Pavlidou E, Polychroniadis EK. SEM observation and differential scanning calorimetric studies of new and sterilized nickel-titanium rotary endodontic instruments. J Endod 2006;32:675–9.
21. Toro A, Zhou F, Wu MH, Van Geertruyden W, Misiolek WZ. Characterization of nonmetallic inclusions in superelastic NiTi tubes. J Mater Eng Perform 2009;18: 448–58.
22. LeMay I. Failure mechanism and metallography: a review. In McCall J, French P, eds. Metallography in Failure Analysis. New York: Plenum Press; 1978:1–31.
23. Beremin FM. Cavity formation from inclusions in ductile fracture of a 508 steel. Metallurgical Transaction 1981;12:723–31.
24. Askeland D, Phule P. The Science of Engineering of Materials. 4th ed. Florence, KY: Brooks/Cole-Thompson Learning; 2003.
25. Kim HC, Yum J, Hur B, Cheung GS. Cyclic fatigue and fracture characteristics of ground and twisted nickel-titanium rotary files. J Endod 2010;36:147–52.
26. Alapati SB, Brantley WA, Svec TA, Powers JM, Nusstein JM, Saehn GS. SEM observations of nickel-titanium rotary endodontic instruments that fractured during clinical use. J Endod 2005;31:40–3.
27. Alexandrou G, Chrissafis K, Vasiliadis L, Pavlidou E, Polychroniadis EK. Effect of heat sterilization on surface characteristics and microstructure of Mani NRT rotary nickel-titanium instruments. Int Endod J 2006;39:770–8.
28. Bonaccorso A, Schäfer E, Condorelli GG, Cantatore G, Tripi TR. Chemical analysis of nickel-titanium rotary instruments with and without electropolishing after cleaning procedures with sodium hypochlorite. J Endod 2008;34:1391–5.